King Saud University

Arabian Journal of Chemistry

www.ksu.edu.sa
www.sciencedirect.com

ORIGINAL ARTICLE

Synthesis and antioxidant study of new polyphenolic hybrid-coumarins

CrossMark

Karina Pérez-Cruz [a,c], **Mauricio Moncada-Basualto** [b,d], **Javier Morales-Valenzuela** [e], **Germán Barriga-González** [f], **Patricio Navarrete-Encina** [c], **Luis Núñez-Vergara** [a,1], **J.A. Squella** [a], **Claudio Olea-Azar** [b,*]

[a] *Laboratory of Bioelectrochemistry, Faculty of Chemical and Pharmaceutical Sciences, University of Chile, Sergio Livingstone Polhammer 1007, Independencia, Santiago, Chile*
[b] *Laboratory of Free Radicals and Antioxidants, Faculty of Chemical and Pharmaceutical Sciences, University of Chile, Sergio Livingstone Polhammer 1007, Independencia, Santiago, Chile*
[c] *Laboratory of Applied Organic Synthesis, Faculty of Chemical and Pharmaceutical Sciences, University of Chile, Sergio Livingstone Polhammer 1007, Independencia, Santiago, Chile*
[d] *Laboratory of Carbohydrate, Faculty of Chemistry and Biology, University of Santiago of Chile, Libertador Bernardo O'Higgins 3363, Estación Central, Santiago, Chile*
[e] *Department of Sciences and Pharmaceutical Technologies Faculty of Chemical and Pharmaceutical Sciences, University of Chile, Sergio Livingstone Polhammer 1007, Independencia, Santiago, Chile*
[f] *Department of Chemistry, Faculty of Basic Science, University Metropolitan of Science of Education, J. P. Alessandri 774, Ñuñoa, Santiago, Chile*

Abstract   The antioxidant capacity of hydroxylated coumarins and hydroxybenzoic acids has been widely described. However, there is little information on the antioxidant activity when both systems are functionalized. In this work, new hybrid compounds synthesis with a common coumarin scaffold and hydroxybenzoic acids is described. Their antioxidant capacity was evaluated against reactive oxygen species (ROS) using oxygen radical absorbance capacity-fluorescein (ORAC-FL), electron spin resonance (ESR) spin trapping, quenching of superoxide anion, cellular antioxidant activity (CAA) and a ferric reducing ability of plasma (FRAP assay). Additionally, the local reactivity indicator (Fukui index) was calculated to discriminate different reactive sites in the new molecules in which the oxidative process occurs. Likewise, the BDE values were calculated in order to obtain information about the antioxidant capacity for HAT mechanisms. The insertion of organic

---

* Corresponding author.
  E-mail address: colea@uchile.cl (C. Olea-Azar).
[1] We dedicate this work to Professor Luis Núñez-Vergara who passed away in the course of this investigation.
Peer review under responsibility of King Saud University.

phenols in a simple coumarin structure produced new derivatives with an improved antioxidant capacity in relation to coumarin 1a. For compound 3c, a synergy phenomenon in ORAC-FL and the FRAP test was observed. For compound 3b, this phenomenon was observed in the superoxide scavenging test. According to the CAA assay results, the activity of the new compounds is limited to those oxidative processes in lipophilic media (e.g., bio membranes).

1. Introduction

Polyphenols are a widely distributed family of compounds in the vegetable kingdom and perform plant secondary metabolites functions, e.g., UV sunscreens, pigments, signal compounds, growth regulators, and defence mechanisms (phytoalexins, Lattanzio et al., 2009). Their biological activity includes anti-inflammatory, cardio protective, vasodilatory, anti-aging, anti-carcinogenic and anti-microbial properties (Xia et al., 2010; Dua et al., 2013; Cimino et al., 2012; Keerthi et al., 2014). Several studies report the antioxidant polyphenolic properties (Pulido et al., 2000; Noguer et al., 2014; Gülçin, 2006; Li et al., 2011) and their human health effect (Pereira et al., 2014). Jeong et al., 2011 studied an *Erigeron annuus* buthanolic extract with an caffeic acid content, which showed neuroprotective and antioxidant effects on neuronal cells.

Coumarins (2H-1-benzopyran-2-one) are substances in seeds, roots and leaves of plants. Natural and synthetic coumarins have been applied in cosmetics (Abernethy, 1969; Ma et al., 2015), food additives (Wang et al., 2013), and agriculture (Lopes et al., 1995). These compounds have well-known biological activities such as anticoagulant, anti-inflammatory, antifungal, antitumors, hepato-protective, ulcerogenic, anti-HIV and an interesting antioxidant activity (Asif, 2014; Kale and Patwardhan, 2014; Jayashree et al., 2014; Kostova, 2006; Kim et al., 2008; Payá et al., 1992, 1996). Regarding the latter property, Payá et al., 1994, studied a mono and dihydroxylated coumarin series towards reactive oxygen species (ROS). They found that simple *ortho* hydroxyl derivatives are radical inhibitors in the lipid peroxidation process. The authors also observed that dihydroxy coumarins could scavenge superoxide in human leucocytes. This topic is interesting because several pathologies such as hypertension, atherosclerosis, diabetes mellitus, cardiovascular pathologies and others are closely linked to the cell redox imbalance (Valko et al., 2007).

Most human diseases (e.g., cancer, diabetes, and neurodegenerative diseases) are complex and multifactorial. Several investigations in the literature focused on new multi-target drug development, which implies active pharmacophores incorporation in one scaffold (Meunier, 2008; Lazar et al., 2004; Teiten et al., 2014). New hybrids have been successfully tested and proposed, such as potential drug candidates, e.g., quinoline and trioxaquine derivatives against malaria (Kouznetsov and Gómez-Barrio, 2009; Chauhan et al., 2010), mustard derivatives that are designed to be similar to anticancer drugs (Xu et al., 2014) and nano-hybrid structures for drug delivery improvement (Allen et al., 2015). Sandhu et al., 2014, describe several examples of hybrid coumarin derivatives with multifunctional characteristics to improve their therapeutic profile. Another study reports stilbene-coumarin synthetic structures that were assayed towards tumoral activity (Belluti et al., 2010).

Vázquez-Rodríguez et al., 2013, described a coumarin-chalcone hybrid synthesis with better antioxidant properties than catechin, quercetin and simple coumarin skeleton. Similarly, Matos et al., 2015, synthesized new coumarin-resveratrol compounds with an interesting antioxidant profile towards oxygen reactive species. Furthermore, these compounds can reduce the ROS (reactive oxygen species) generation in RAW 264.7 cells.

These facts prompted us to design a synthetic route of coumarin functionalized scaffold with hydroxyl benzoic acids (known antioxidant frameworks (Kakkar and Bais, 2014; Wojdyło et al., 2007; Li et al., 2011) and perform different antioxidant assays to study new derivative antioxidant properties.

2. Experimental section

2.1. Synthesis

The common scaffold 1a was obtained by mixing 31 mmol of pyrogallol with 4-chloroethylacetoacetate in equimolar ratio. Cold H_2SO_4 (25 mL) was added and stirred for 1 h in an ice-water bath. The product was poured into an ethanol-ice water mixture to obtain a solid, which was washed with water and recrystallized in an ethanol/H_2O mixture. The common scaffold 1a hydroxyl group was protected with acetic anhydride in acidic media.

2.2. Chemicals

Gallic acid, protocatechuic acid, DBU (1,8-diazabicyclo[5.4.0] undec-7-ene), 4-chloroethylacetoacetate, fluorescein, AAPH (2,2′-azobis(2-methylpropionamidine)dihydrochloride), (DMPO (5,5-dimethyl-1-pyrroline-N-oxide), tetrabuthyl ammonium hexaphluorophosphate (Bu_4NPF_6) 99.99%, 2′,7′-dichlorodihydrofluorescein diacetate (DCFH-DA), were analytical grade and purchased from Sigma-Aldrich, USA. Caffeic acid, 2,4,6-tris(2-pyridyl)-s-triazine (TPTZ), $CH_3COONa\cdot3H_2O$, $FeCl_3\cdot6H_2O$, NaOH, KH_2PO_4, hydrogen peroxide (30%), N,N-dimethylformamide (DMF), dimethylsulfoxide (DMSO), orthophosphoric acid, acetic acid (glacial), acetic anhidrid, pyrogallol, chloroform, ethanol, acetone, were analytical grade and were obtained from Merck KGaA, Germany. Ultrapure water was from NanoPure water equipement, Barnstead, Thermo Scientific USA. Methanol and HCl (37%) were analytical grade and purchased from J. T. Baker, USA. Extra pure nitrogen (99.999%) was purchased from Linde Gas, Chile. Cell line EA. hy 926 (ATCC CRL-2922) was purchased from American Type Cell Culture (ATCC).

2.2.1. General procedure

Esterification reactions were performed with protected hydroxyacids (gallic acid, protocatechuic acid, caffeic acid) which were previously activated with DBU (1,8-diazabicyclo[5.4.0]undec-7-ene). The hydroxyl protection was cleaved by mild basic saponification. The acylated acid derivative (2b-d) (3.2 mmol) was mixed with DBU in a 1:1 ratio in 10 mL of dry DMF (N,N-dimethylformamide). The mixture was stirred for 30 min at room temperature. Protected coumarin 2a (3.2 mmol) was added to the mixture and maintained at 50 °C for 3.5 h with stirring, and $CaCl_2$ filled the drying tube in the Erlenmeyer flask to avoid moisture. The reaction mixture was poured into water; the solid formed was filtered and

vacuum dried. Compound deacylation was performed at room temperature for 3 h in a nitrogen atmosphere in a mixture of acetone (12 mL), methanol (8 mL) and saturated solution of $NaHCO_3$ (14 mL). The product was concentrated in vacuum and acidified with HCl. An ivory-coloured solid was formed, which was filtered, washed carefully with distilled water (to eliminate water-soluble residues) and dried. Finally, it was washed carefully with three 10 mL portions of boiling $CHCl_3$ (to eliminate non-polar impurities) to afford the new compounds (**3a-c**). The compounds were characterised with ^{1}H NMR and ^{13}C NMR spectroscopy using a 300 MHz spectrometer (Bruker, WM 300). New hybrid structures were characterised by mass spectroscopy (ESI-IT Esquire 4000 (Bruker Daltonik GmbH, Germany). Considering that the compounds **3a-c** are new (they are not commercially available), they were tested by HPLC-DAD (data not shown) and we obtained that compounds were around 90%.

2.2.2. 4-Chlorometyl-7,8-dihydroxycoumarin (1a) (Aguirre et al., 2016; Campos-Toimil et al., 2002; Gümüş et al., 2010)

Yield: 47%, m. p.: 202–204 °C (195 °C lit, Sharma et al., 2011), ivory needles. ^{1}H NMR (DMSO-d_6, δ ppm): 4.93 (s, 2H, −CH_2−), 6.41 (s, 1H, =CH-coumarin); 6.86 (d, 1H, $J = 8.5$), 7.17 (d, 1H, $J = 8.5$), 9.42 (s, 1H, OH), 10.22 (s, 1H, OH). ^{13}C NMR (DMSO d_6, δ ppm): 41.9, 110.5, 111.3, 112.7, 115.9, 132.8, 143.6, 150.2, 151.8, 160.5. M.f.: $C_{10}H_7O_4Cl$.

2.2.3. 4-Chlorometyl-7,8-diacetoxycoumarin (2a)

Yield: 68%, m. p.: 157–159 °C, white needles. ^{1}H NMR (DMSO-d_6, δ ppm): 2.35 (s, 3H, −CH_3), 2.41 (s, 3H, −CH_3), 5.06 (s, 2H, −CH_2−), 6.74 (s, 1H, =CH-coumarin), 7.39 (d, 1H, $J = 8.78$), 7.83 (d, 1H, $J = 8.78$). ^{13}C NMR (DMSO-d_6, δ ppm): 19.4, 19.9, 39.8, 40.7, 114.7, 115.5, 118.7, 122.4, 129.4, 144.6, 145.9, 150, 157.9, 167.5. M.f.: $C_{14}H_{11}O_6Cl$.

2.2.4. 3,4-Diacetoxycinnamic acid (2b) (Touaibia and Guay, 2011)

Yield: 56%, m. p: 158–161 °C (190–192 °C lit.), white solid. ^{1}H NMR (acetone-d_6, δ ppm): 2.15 (s, 3H, −CH_3), 2.16 (s, 3H, −CH_3), 6.38–6.43 (d, 1H, $J = 15.9$) 7.17–7.20 (d, 1H, $J = 8.7$), 7.47–7.56 (m, 3H, ArH, −CH=CH-trans). ^{13}C NMR (acetone-d_6, δ ppm): 20, 20.1, 119.8, 123.3, 124.5, 126.8, 133.6, 143.2, 143.4, 144.39, 167, 168.1, 168.2. M.f.: $C_{13}H_{12}O_6$.

2.2.5. 3,4,5-Triacetoxibenzoic acid (2c) (Gazit et al., 1989)

Yield: 66%, m. p.: 158–160 °C (163 °C, lit, Carvalho et al., 2016) white solid. ^{1}H NMR (acetone-d_6, δ ppm): 2.17 (s, 6H, −CH_3), 2.19 (s, 3H, −CH_3), 7.67 (s, 2H, ArH). ^{13}C NMR (acetone-d_6, δ ppm): (2C, −CH_3, 18.7), (2C, −C=O, 19.1), (2C_{arom}, 121.6), 127.9, 138.6, (2C 143.4), 164.3, 166, 167.9. M.f.: $C_{13}H_{12}O_8$.

2.2.6. 3,4-Diacetoxybenzoic acid (2d). (LeBlanc et al., 2012)

Yield: 61%, m. p: 155–158 °C (157–158 °C, lit. Link et al., 1929), white solid. ^{1}H NMR (acetone-d_6, δ ppm): 2.17 (s, 6H, -CH_3), 7.24–7.27 (d, 1H-ArH, $J = 8.5$), 7.81–7.84 (dd, 2H ArH, $J = 8.2$, $J = 1.9$). ^{13}C NMR (acetone-d_6, δ ppm):

19.1, 19.1, (2C, 123.3), 124.5, 127.3, 128.4, 142, 145.9, 164.9, 167. M.f.: $C_{11}H_{10}O_6$.

2.2.7. 4-Methyl-(3,4-dihydroxycinnamoate)-7,8-dihydroxycoumarin (3a)

Yield: 37%, m. p.: 246–249 °C, opaque yellow solid. ^{1}H NMR (DMSO-d_6, δ ppm): 5.41 (s, 2H, −CH_2−), 6.21 (s, 1H, −CH-coumarin), 6.42–7.63 (m, 5H-ArH, −CH=CH-trans), 9.1(s, −OH), 9.4 (s, −OH), 9.7 (s, −OH), 10.2 (s, −OH). ^{13}C NMR (DMSO d_6, δ ppm): 61.5, 108.2, 110.4, 112.9, 113.5, 115.3, 115.5, 116.2, 122.3, 125.7, 132.9, 143.9, 146.1, 146.9, 149.2, 150.3, 151.7, 160.6, 166.5. ESI-MS m/z: 371[M + H]$^+$, 369[M−H]$^-$, 181[M + H]$^+$, 163[M−H_2O + H]$^+$, 145[M−H_2O + H]$^+$, 135[M−HCOOH + H]$^+$, 179 [M−H]$^-$, 161[M−H_2O-H]$^-$, 135[M-CO_2-H]$^-$. Anal. Calcd. for $C_{19}H_{14}O_8$: C, 61.62; H, 3.81. Found: C, 61.65; H, 3.83

2.2.8. 4-Methyl-(3,4,5-dihydroxybenzoate)-7,8-dihydroxycoumarin (3b)

Yield: 46%, m. p.: 230 °C (dec), opaque yellow solid. ^{1}H NMR (DMSO-d_6, δ ppm): 5.46 (s, 2H, −CH_2−), 6.19 (s, 1H, −CH-coumarin), 6.82–7.12 (m, 4H, ArH). ^{13}C NMR (DMSO d_6, δ ppm): 6.92, 108.21, 109.14, 110.41, 112.95, 115.33, 118.85, 132.92, 139.49, 143.94, (2C_{arom}) 146.20, 150.24, 151.84, 160.55, 165.55, 167.93. ESI-MS m/z: 361[M + H]$^+$, 359 [M−H]$^-$, 171[M + H]$^+$, 153[M−H_2O + H]$^+$, 125[M−CO_2H + H]$^+$, 169 [M−H]$^-$, 125[M−CO_2−H]$^-$. Anal. Calcd. for $C_{17}H_{12}O_9$: C, 56.67; H, 3.36. Found: C, 56.57; H, 3.38

2.2.9. 4-Methyl-(3,4-dihydroxybenzoate)-7,8-dihydroxycoumarin (3c)

Yield: 73%, m. p.: 250 °C (dec), opaque yellow solid. ^{1}H NMR (DMSO-d_6, δ ppm): 5.48 (s, 2H, −CH_2−6.19 (s, 1H, −CH-coumarin), 6.85–7.4 (m, 5H-ArH). ^{13}C NMR (DMSO d_6, δ ppm): 61.42, 107.74, 109.88, 112.42, 114.81, 115.51, 116.26, 119.57, 122.18, 132.40, 143.43, 145.20, 149.72, 150.96, 151.27, 160.01, 164.90. ESI-MS m/z: 345 [M + H]$^+$, 343 [M−H]$^-$, 137 [M−H_2O + H]$^+$, 109 [M−HCOOH + H]$^+$, 153 [M−H]$^-$, 108 [M−CO_2−H]$^-$. Anal. Calcd. for $C_{17}H_{12}O_8$: C, 59.31; H, 3.51. Found: C, 59.13; H, 3.57

2.3. Antioxidant assays

2.3.1. Evaluation of ORAC-FL activity

Analyses were performed in a Synergy HT Multi-Detection Microplate Reader from BioTek Instruments, Inc. (Winooski, USA) using polystyrene a 96-well plate, (Nunc, Denmark). Fluorescence was measured from the top at an excitation wavelength of 485/20 nm and an emission wavelength of 528/20 nm. The Gen5 software controlled the plate reader. The reaction was performed at 37 °C in PB (phosphate buffer solution pH = 7.4), and the final volume was 200 μL. Fluorescein was prepared in a buffer solution (40 nM). Stock compound solutions were prepared in ethanol and diluted in PB to obtain the working solutions. The stock solutions were placed in each well of a 96-well plate. The working concentrations that enabled accurate separation of fluorescence decay curves were 0.2–10.9 μM. The mixture was pre-incubated for 15 min at 37 °C before the AAPH solution was added (final concentration 18 mM). The microplate was immediately

placed in the reader and automatically shaken before each reading. The fluorescence was recorded every 1 min for 120 min. A control assay with fluorescein, AAPH, and PB (instead of the antioxidant solution) was performed for each assay. Trolox was used as the standard antioxidant in a final concentration range of 3.0–20.0 µM. The inhibition capacity was expressed as ORAC values and quantified by integrating the area under the curve (AUC_{net}). The area under the fluorescence decay curve (AUC) was calculated by integrating the decay of the fluorescence, where F_0 is the initial fluorescence at 0 min, and F is the fluorescence at a certain time. The AUC_{net} corresponding to the sample was calculated by subtracting the AUC that corresponded to the control assay.

2.3.2. Evaluation of OH· scavenging by ESR

The ESR (electron spin resonance) spectra were recorded in the X band (9.7 GHz) using a Bruker ECS 106 spectrometer with a rectangular cavity and 50-kHz field modulation, which was equipped with a high-sensitivity resonator at room temperature. The spectrometer conditions were: microwave frequency 9.81 GHz; microwave power 20 mW; modulation amplitude 0.91 G; receiver gain 59 db; time constant 81.92 ms; conversion time 40.96 ms. The scavenging activity of each derivative was estimated by comparing the DMPO-OH adduct signals in the antioxidant-radical reaction mixture and the control reaction at the identical reaction time. The scavenging activity is expressed as the scavenging percentage of hydroxyl radical. The compound reactivity against hydroxyl radical was investigated using the non-catalytic Fenton type method. The samples were prepared as follows: 100 µl of DMF and 50 µl of NaOH (25 mM) were mixed. Then, 50 µl of DMPO (5,5-dimethyl-1-pyrroline-N-oxide, 30 mM final concentration), 50 µl of sample (20 mM in DMF) and 50 µl of hydrogen peroxide (30%) were sequentially added. The mixture was put into an ESR cell, and the spectrum was recorded after five minutes of reaction.

2.3.3. Evaluation of the ferric reducing antioxidant power (FRAP)

2.3.3.1. Reagent solutions. Acetate buffer: $CH_3COONa \cdot 3H_2O$ (1.55 g) was completely dissolved in ultrapure water. Acetic acid (8 mL) was added and completed to 500 mL. The pH value was adjusted to 3.6 with concentrated NaOH.

Phosphate buffer pH 7.4: NaOH solution (80 mL, 0.1 M) was mixed with KH_2PO_4 solution (100 mL, 0.1 M) and stirred to homogenize.

HCl 40 mM solution: 167 µL of HCl solution (12 M) was added to a 50 mL volumetric flask, and the volume was completed with ultrapure water.

TPTZ (2,4,6-tris(2-pyridyl)-s-triazine) solution: 79.7 g of TPTZ reactive was completely dissolved in 25 mL HCl solution (40 mM). This solution was light protected and freshly prepared.

$FeCl_3$ solution: 0.054 g of $FeCl_3 \cdot 6H_2O$ was dissolved in ultrapure water (10 mL) and homogenized.

FRAP reagent: The acetate buffer : TPTZ solution : $FeCl_3$ solution was mixed in a 10:1:1 ratio. This mixture was carefully homogenized and light protected.

2.3.3.2. FRAP assay. First, 150 µL of sample solution was mixed in an amber flask with ultrapure water (450 µL) and the FRAP reagent (950 µL). The solution was stirred; then, its absorbance was measured at room temperature. Stock solutions were prepared in ethanol and diluted with a phosphate buffer to afford sample solutions in the range of 15–58 µM. The FRAP values were expressed as Trolox equivalents/10 µM sample.

2.3.4. Superoxide anion assay by cyclic voltammetry (CV)

The superoxide radical anion O_2^- was electrogenerated by reducing dissolved oxygen in dry DMF. The electrochemical cell consisted of three electrodes: glassy carbon as the working electrode ($a = 0.03$ cm^2); Ag/AgCl (3 M, KCl) as the reference electrode, which was separated from the solution by a salt bridge that contained 0.2 M Bu_4NPF_6 (tetrabutylammonium hexaphluorophosphate) in the analytical-grade DMF (Sigma-Aldrich); a Pt wire counter electrode. The working solutions were in DMF (10 mL) with a supporting electrolyte (Bu_4NPF_6, 0.2 M) and saturated with air. Stock solutions (0.1 M) were prepared for each compound in DMF, and aliquots were added to the 10 mL oxygenated solution to increase the antioxidant concentration. After each aliquot addition, the voltammograms were recorded at a scan rate of 0.1 V/s; the potential window was from 0 V to −1 V. Before each measurement, the working electrode was polished to a mirror finish with alumina powder (0.3 µm and 0.05 µm) and carefully washed. The antioxidant activity was assessed from the change in anodic current of the voltammograms in the absence and presence of the derivatives, using pertinent mathematical formulations. The relative decrease in anodic peak (Le Bourvellec et al., 2008) was expressed as $(Ipa° − Ipa^S)/Ipa°$, where Ipa° is the current peak in the oxidative scan in the absence of a substrate, and Ipa^S is the current peak in the oxidative scan in the presence of a substrate (Fig. 1). The CV measurements were performed in a Metrohm instrument with a 694VA stand convertor and a 693VA processor.

2.3.5. Evaluation of cellular antioxidant activity

The cellular antioxidant activity (CAA) was evaluated in EA. hy 926 (ATCC CRL-2922) cells using 2′,7′-dichlorodihydro fluorescein diacetate (DCFH-DA, 20 µM) as fluorescent probe (Wolfe and Liu, 2007). The cells were plated in white sterile polystyrene flat-bottom 96-well microplates at concentration
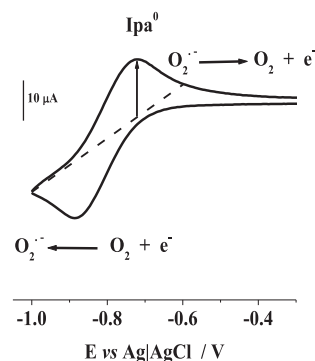

Figure 1 CV for the superoxide anion formation in the glassy carbon electrode surface. Example for compound **1a**. 0.1 V/s, 2 mM in DMF + Bu_4NPF_6, 0.2 M.

of 50,000 cells per well and incubated for 24 h at 37 °C in RPMI 1640 culture medium. The cells were washed with phosphate buffer saline (PBS, pH 7.4) and incubated for 1 h with 100 mL of RPMI 1640 containing the fluorescent probe (20 μM). This medium was discarded and carefully washed with PBS solution. Studied compounds (solutions in buffer/dimethylsulfoxide (DMSO), containing less than 1% DMSO) were added in concentrations 1 μM and 10 μM. After 1 h incubation, the medium was discarded and the cells were gently washed with PBS. Then they were incubated with AAPH (final concentration 600 μM in PBS). Fluorescence was measured immediately after AAPH addition at 37 °C in a Synergy HT Multi-Detection Microplate Reader, from BioTek Instruments, Inc. (Winooski, USA) using an excitation wavelength of 485 nm and an emission wavelength of 538 nm. Evaluation was performed every minute for 1 h. Cellular antioxidant capacity (CAA) was calculated as follows in Eq. (1):

$$\% \, CAA = 100 - \left(\int_{sample} \Big/ \int_{control} \right) * 100 \tag{1}$$

$\int_{sample}$ = sample area under curve
$\int_{control}$ = control area under curve

2.3.6. High-performance liquid chromatography (HPLC)

The HPLC system was equipped with Agilent system 1100 and a photodiode array detector. HPLC analysis was performed using an ODS Hypersyl (5 mm-particle size, 25 mm × 4.6 mm i.d.) column from Agilent. All experiments were carried out at 20 °C of column temperature. The mobile phase consisted of 0.2% orthophosphoric acid solution-acetonitrile (35:65, v/v) with isocratic elution at a flow-rate of 1 mL/min. The diode array detector was operated at 329 nm (compounds 1 and 9), 265 nm (compound 10) and 262 nm (compound 11) with 4 nm of bandwidth. Injection volume was set at 30 μL.

2.4. Computational methods

2.4.1. Fukui index

The density functional theory (DFT) is currently an important approach to characterise the behaviour of molecules using computational methods. The use of the conceptual density functional theory (DFT) has emerged as an important tool, which enables us to study the reactivity of different compounds and reactions using various tools. The reactivity is a fundamental concept of great importance because it enables us to understand interactions that occur during a reaction mechanism.

Fukui function is defined in terms of the derivative of the electron density ($\rho(r)$) with respect to the number of electrons (N). Using the appropriate Maxwell relation, the following equality can be written:

$$f(\mathbf{r}) = \left(\frac{\partial \rho(\mathbf{r})}{\partial N} \right)_{v(r)} = \left[\frac{\delta \mu}{\delta v(\mathbf{r})} \right]_N \tag{2}$$

Then, if the number of electrons corresponds to a discrete variable, the right and left derivatives of the electron density with respect to N enable us to obtain two different definitions of Fukui functions:

$$f^+(\mathbf{r}) = \left(\frac{\partial \rho(\mathbf{r})}{\partial N} \right)_{v(r)}^+ = \rho_{N+1}(\mathbf{r}) - \rho_N(\mathbf{r}) \tag{3}$$

$$f^-(\mathbf{r}) = \left(\frac{\partial \rho(\mathbf{r})}{\partial N} \right)_{v(r)}^- = \rho_N(\mathbf{r}) - \rho_{N-1}(\mathbf{r}) \tag{4}$$

where the first expression indicates the reactivity to a nucleophilic attack, and the second indicates the reactivity to an electrophilic attack. It should be noted that $\rho N + 1(r)$, $\rho N(r)$ and $\rho N - 1(r)$ correspond to the electronic density for the system with $N + 1$, N and $N - 1$ electrons (Martínez-Araya et al., 2013; Baerends and Ros, 1978).

We calculated the Fukui function using the densities of frontier molecular orbitals (FMOs), $\rho HOMO(r)$ and $\rho LUMO(r)$ respectively. We used this approximation due to has been demonstrated that when orbital relaxation is irrelevant exists a direct relation between Fukui functions and the density of the appropriate FMO (Parr and Yang, 1984; Yang et al., 1984). This allows avoiding the calculation of cationic (N − 1) and anionic (N + 1) systems. We can also define a third Fukui function related to the radical attack, which is denoted as $f^0(r)$, based on the two afore-mentioned Fukui functions as follows (Demircioğlu et al., 2015):

$$f^0(\mathbf{r}) = \frac{1}{2} \left(f^+(\mathbf{r}) - f^-(\mathbf{r}) \right) \tag{5}$$

Computational calculations were performed to rationalize the experimental results using the Density Functional Theory (DFT, Baerends et al., 1973; Baerends and Ros, 1978; Boerrigter et al., 1988; Te Velde and Baerends, 1992). These calculations were performed using the Gaussian '09 software package (Frisch et al., 2009). All structural optimisations were carried out using B3LYP hybrid functional. The basis set 6-31 + +G(d,p) were used for closed and open shell structures at the corresponding ground electronic states (Francl et al., 1982). For all optimised structured the frequencies were computed. The frequencies confirm that the geometries obtained correspond to minima (Bauschlicher and Langhoff, 1999). All calculations were performed in the gas-phase and considering the solvent effects. Condensed Fukui functions were obtained using single point one-determinantal calculation performed with Fukui software (Chamorro and Pérez, 2005).

2.4.2. Bond dissociation energies (BDE)

BDE was calculated the for each OH group of these new polyphenolic hybrid-coumarins using the following reaction scheme:

$$R - H \rightarrow R^\cdot + H^\cdot \tag{6}$$

From the calculated energies for each molecule, its radical and the isolated radical form of H atom, we are able to obtain the BDE as:

$$BDE = E_{RH} - (E_{R^\cdot} + E_{H^\cdot}) \tag{7}$$

We use the exact energy for H radical as −0.5 hartrees (Kozlowski et al., 2007; Bauschlicher and Langhoff, 1999).

3. Results and discussion

3.1. Chemistry

Coumarin derivatives **1a**, **3a-c** were synthesized according to the outlined Scheme 1. Step 1: synthesis of the common scaffold 4-chloromethyl-7,8-dihydroxycoumarin **1a**. Step 2: protection of catechol groups that form **2a-d** compounds. Steps 3, 4: hybrid compound formation and deacylation of hydroxyl groups to produce **3a-c**. Step 1 was accomplished using the well-known Pechmann coumarin synthesis (Sethna and Narsinh, 1944; von Pechmann, 1884). Step 2: hydroxyl groups were protected as acyl ester derivatives (Furniss et al., 1948; Touaibia and Guay, 2011). Step 3: acylated acid derivatives (**2b-d**) were mixed with DBU (1,8-diazabicyclo[5.4.0]undec-7-ene, Ono et al., 1978) in dry DMF (N,N-dimethylformamide), protected halo-coumarin (**2a**) was added to the mixture to form acylated hybrid compounds. Step 4: the deacylation was performed by mild basic saponification in an inert atmosphere to obtain the desired polyphenolic derivatives.

3.2. Antioxidant capacity studies

The antioxidant capacity of coumarin derivatives was evaluated towards the biologically relevant ROS: peroxyl (ROO$^\bullet$), hydroxyl (OH$^\bullet$) and superoxide anion (O$_2^{\bullet-}$) radicals. Different assays including oxygen radical absorbance capacity-fluorescein (ORAC-FL), ferric reducing ability of plasma (FRAP), spin trapping assay and cellular antioxidant activity (CAA) were selected to achieve the goals. Trolox (($\pm$)-6-hydroxy-2,5,7,8-tetramethylchroman-2-carboxylic acid), which is a vitamin E hydro-soluble derivative, was the standard. All measurements were performed in triplicate, and the values are expressed as the mean $\pm$ SD and are accompanied by the number of observations (n). Statistical analysis was performed using a R^2 parameter, Chi-Square test or one-way ANOVA and comparisons between groups were performed by Tukey's multiple comparison test. $p < 0.05$ was considered significant. Data processing was performed using the Origin Pro 8 software (Origin Lab Corporation, USA).

3.2.1. Evaluation of ORAC-FL

We obtained kinetic profiles in fluorescein consumption by peroxyl radical generated from the induced AAPH pyrolysis at 37 °C (Fig. 2). The obtained oxygen radical absorbance capacity-fluorescein (ORAC-FL) indices are shown in Table 1.

Fig. 2 illustrates the fluorescein (FL) oxidation results. The fluorescent probe was protected by antioxidant compounds (lag time) that competed with peroxyl radicals (Cao et al., 1993; Ou et al., 2001) formed by 2,2′-azobis(2-methylpropionamidine)dihydrochloride (AAPH) thermolysis at 37 °C. AUC$_{net}$ (net area under curve) was calculated (Fig. 3). In all experimental ranges, we observed a linear correlation to AUC$_{net}$ *vs* substrate concentration (Fig. 4).

Compounds **3a**, **3b** and **3c** presented better ORAC-FL values than Trolox and two or three times more than **1a**. Thus, the polyphenol inclusion in the coumarin scaffold contributed to the heterocycle antioxidant capacity. **3a** and **3c** derivatives had similar ORAL-FL values, which indicates that the double
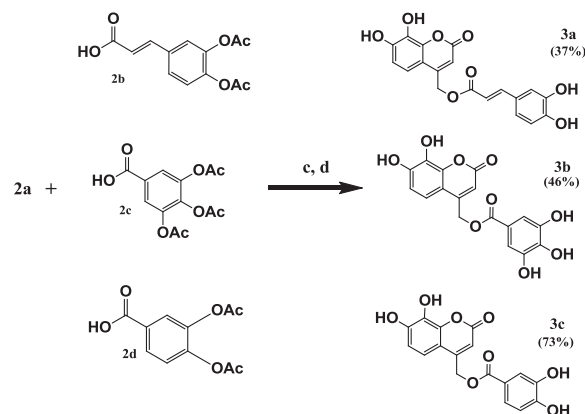
Step 1

a: H$_2$SO$_4$, 1 h, ice bath.

Step 2.
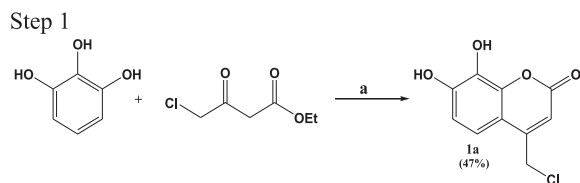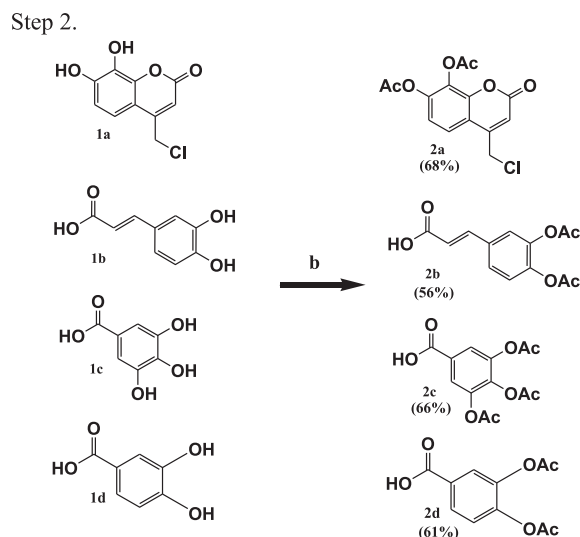
b: NaOH, acetic anhydride, 30 min., ice bath (caffeic acid **1b**); H$_2$SO$_4$, acetic anhydride, 30 min. (coumarin **1a** and benzoic acids **1c-d**).

Steps 3 and 4.

c: DBU, dry DMF, 3.5 h., 50 °C. d: NaHCO$_3$, MeOH, acetone, r.t., 3 h, N$_2$ inert atmosphere.

Scheme 1 Coumarin and acid derivatives (**1a**, **2a-d**, **3a-c**) synthetic route.

bond in the **3a** structure does not play a relevant role in the peroxyl scavenging in this methodology.

The antioxidant response of phenolic acids and related derivatives depends on some structural characteristics: (a) the number of position of the –OH substituents in the aromatic ring; (b) alcoxy groups in the ortho position to the hydroxyl
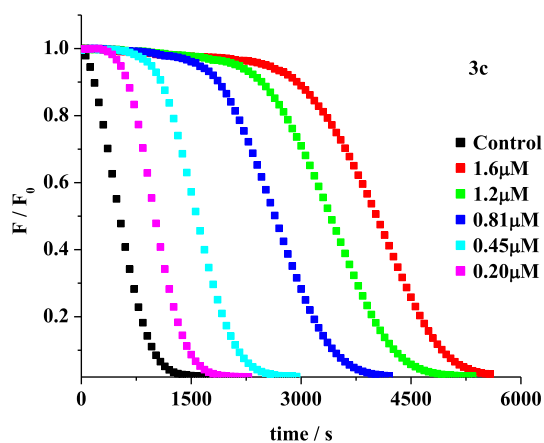
Figure 2 Kinetic profiles of FL consumption to compound **3c** determined by the intensity of the fluorescent probe at 528 nm *vs* incubation time.

Table 1 ORAC–FL values for the studied compounds.

Compound	ORAC-FL index
1a	0.91 ± 0.03
Caffeic acid 1b	3.47 ± 0.10
Gallic acid 1c	3.91 ± 0.09
Protocatchuic acid 1d	0.69 ± 0.01
3a	2.39 ± 0.03
3b	1.74 ± 0.05
3c	2.62 ± 0.04
Trolox	1

All experiments were performed in triplicate. The data are expressed as the mean ± SD.
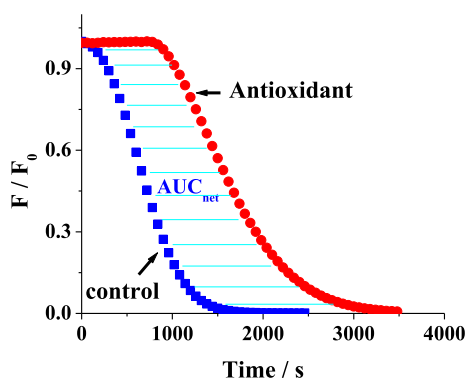
Figure 3 AUC$_{net}$ determination in the ORAC-FL assay.

group; (c) the presence of —CH=CH— and —COOH groups in the structure (Materska and Perucka, 2005). The **3c** derivative showed a synergic behaviour, where its ORAC-FL value (2.62) was higher than their precursors (protocatechuic acid 0.61 and **1a** 0.91). Meanwhile, we observed that caffeic acid and gallic acid had higher ORAC values (3.47 and 3.91, respectively) than derivatives **3a** (2.39) and **3b** (1.74). The cause may be that the ester substituent (hydroxylated coumarin skeleton)
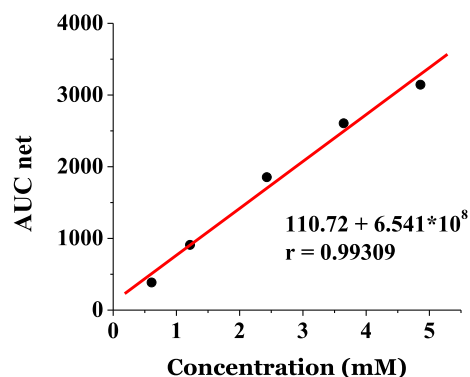

**Figure 4** AUC$_{net}$ *vs* substrate concentration. Compound **3c**.

is a voluminous moiety attached to the acid, which can decrease the system configuration co-planarity. Although esterification can increase the antioxidant capacity in this scaffolds (Rice-Evans et al., 1996; Mura et al., 2014), the structural characteristics are different in our case. For the caffeic acid derivative, we observed that the decrease was not greater than gallic acid because the —CH=CH— spacer between the ring and the coumarin substituent increased the stability by resonance in the phenoxyl radical (ArO·), which is a reaction intermediary (Materska and Perucka, 2005).

The relative antioxidant capacity order was: **gallic acid > caffeic acid > 3c > 3a > 3b > 1a > protocatechuic acid.**

3.2.2. Evaluation of OH· scavenging by ESR

Since its development by Zavoisky in 1940 (Salikhov and Zavoiskaya, 2015), this non-destructive technique, which enables the detection and identification of paramagnetic species in different matrices, have been applied in several investigation fields such as food antioxidants (Polovka, 2006) and tropical parasitic diseases (Olea-Azar et al., 2006). In biomedical sciences, this tool is important in the study of living systems where different radical species promote cell oxidative damage (Spasojević et al., 2011).

The hydroxyl-scavenging ability was assessed by a noncatalytic and competitive Fenton system that uses DMPO (5,5-dimethyl-1-pyrroline-N-oxide) as the spin trap in basic media without an Fe^{2+} catalyst for the radical formation (Yoshimura et al., 1999, Eq. (7)). The spin trap reacts with hydroxyl radicals to generate a spin adduct that shows a control signal, which is quantified by electron spin resonance (ESR). Fig. 5 illustrates four hyperfine lines because of the DMPO-OH adduct formation. In our experiments, the obtained control ESR spectrum was the mixture of DMPO + DMF + NaOH + H_2O_2. (Fig. 6 in black).

$$2H_2O_2 + OH^- \rightarrow OH^· + O_2^- + 2H_2O \qquad (8)$$
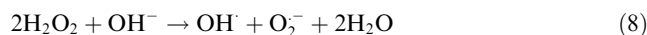
The ESR spectra for all compounds show that the DMPO-OH adduct signal decreased by almost 100% to produce a triplet with coupling constants of approximately 14 Gauss, which implies the DMPO oxidation. This response was observed for all compounds (Fig. 6, highlighted in blue).

The radical-scavenging values (Table 2) indicate that compounds **3a** and **3b** were similar and better than the coumarin moiety with values of approximately 99%. Derivative **3c** had
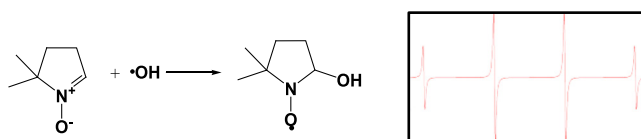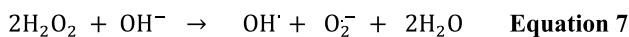
$$2H_2O_2 + OH^- \rightarrow OH^{\cdot} + O_2^{-} + 2H_2O \qquad \textbf{Equation 7}$$

Figure 5 Spin adduct [DMPO-OH.] formation in the spin trapping reaction. Simulated ESR spectra (right).
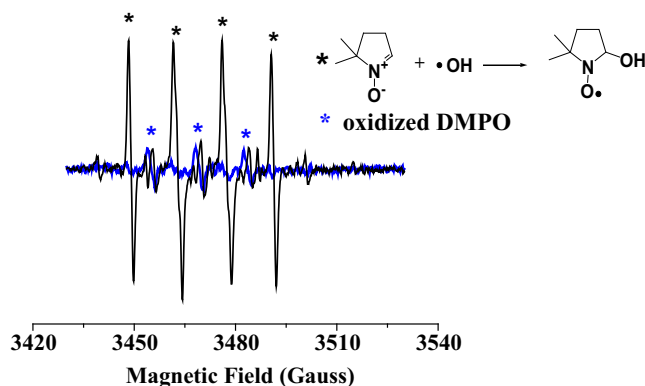

Figure 6 ESR spectra for protocatechuic acid; the black line represents the sample signal before the compound addition.

Table 2 Percentage of scavenging of hydroxyl radicals, which was calculated for the studied compounds.

Compound	% Scavenging of OH· radical[a]
1a	92.3 ± 7.4
Caffeic acid 1b	98.1 ± 1.8
Gallic acid 1c	98.2 ± 2.5
Protocatchuic acid 1d	98.0 ± 9.9
3a	98.3 ± 2.7
3b	99.5 ± 0.8
3c	92.7 ± 2.9
Trolox[b]	31 ± 2.5

[a] All experiments were performed in triplicate. The data are expressed as the mean ± SD. The scavenging activity of the hydroxyl radical effect was calculated as follows: $[(A_0 - A_x)/A_0] \times 100$, where A_x and A_0 are the double-integral electron spin resonance for the first line of samples in the ESR spectra.
[b] Trolox value was collected from reference Meunier, 2008.

a similar value to begin scaffold **1a** (approximately 92%). All compounds had higher values than Trolox.

Previous studies (Pérez-Cruz et al., 2013) about simple mono-hydroxylated coumarins similar to **1a** showed only a 29% of scavenging compared with the di-hydroxylated derivative **1a.** This difference occurs because of the o-quinone formation after the scavenging of two OH· radicals. Meanwhile, Figueroa et al., 2013, obtained 23% and 56% scavenging in the identical experiment with simple mono-substituted coumarins.

The values in Table 2 show some results that exceeding more than 100% e.g. the compound **1d**; it could be explained because in this assay are formed not only OH· radicals

(Yoshimura et al., 1999), carbon centered radicals are formed too in small quantity which can react simultaneously with the phenolic compound. Pérez-Cruz et al., 2013, reports a set of hydroxycoumarin compounds assayed against reactive oxygen species, they show an example of a dihydroxylated compound with an additional hyperfine pattern in the ESR spectra attributed to DMPO-carbon-centered radical adduct.

Despite the low selectivity and high reactivity of the OH· radical, all compounds can compete with DMPO to scavenge for radicals, which suggests that they are interesting candidates to inactivate OH· (considering that the spin trap DMPO and OH· lifetime is 10^{-9} s). The relative order of the hydroxyl radical scavenging was **gallic acid ∼ caffeic acid ∼ 3b ∼ 3a ∼ 3c ∼ protocatechuic acid > 1a.**

3.2.3. Evaluation of the ferric reducing antioxidant power (FRAP assay)

The ferric reducing ability of plasma (FRAP) is a simple and automated test to measure the ferric reducing ability of antioxidants in different samples such as plasma (Benzie and Strain, 1996), phenolic extracts (Gohari et al., 2011), foods (Bolanos de la Torre et al., 2015) or pure compounds (Biskup et al., 2013). The ferric complex formation and subsequent redox reaction with an antioxidant compound are indicated by a blue complex formation (Scheme 2) with an absorption maximum at 593 nm. This methodology involves a redox reaction between a reductant (hydroxylated compounds) and the oxidant $[Fe(III) (TPTZ)_2]^{3+}$ (ferric 2,4,6-tris(2-pyridyl)-s-triazine). In this assay, the reducing power of the antioxidants reflects the ability of the compounds to maintain the redox status in cells or tissues (Prior et al., 2005).

The activity of the studied compounds is shown in Table 3. Derivatives **3a-c** have higher reducing power than coumarin **1a** with values two to three times higher than their precursor **1a**. The inclusion of phenolic structures (**1b-d**) into the original scaffold produces new compounds with superior reducing capacity. Compounds **3a-c** have more hydroxyl substituents in their structures than the coumarin moiety. Therefore, more active groups can transfer electrons to reduce the ferric salt $[Fe(III) (TPTZ)_2]^{3+}$ and increase the FRAP values (Pulido et al., 2000). This behaviour is related to the degree of hydroxylation and extent of conjugation in polyphenols.

The values of protocatechuic acid and **1a** were 86.8 and 130.2 equiv. Trolox /10 μM, respectively. Their derivative **3c** shows a FRAP value of 262.4 equiv. Trolox /10 μM, which gives a synergistic relationship. Similar to the previous trial, this result shows that the substitution on the coumarin ring with different phenolic groups increases their potential as reductant species in this methodology.

We found a similar behaviour related to the ORAC assay. We observed differences of approximately 476.8 vs 318.2 in the case of gallic acid and 272.7 to caffeic acid vs 205.2 for the **3a** derivative. Carboxylic acid replaced by voluminous ester shows the previously observed effect. Regarding to the activity of the compounds, the relative order was **gallic acid > 3b > caffeic acid > 3c > 3a > 1a > protocatechuic acid.**

3.2.4. Superoxide anion scavenging

A recent review describes an application of the electrochemical techniques in antioxidant capacity studies. Pisoschi et al.

yellow
[Fe(III) (TPTZ)₂]³⁺

blue
[Fe(III) (TPTZ)₂]²⁺
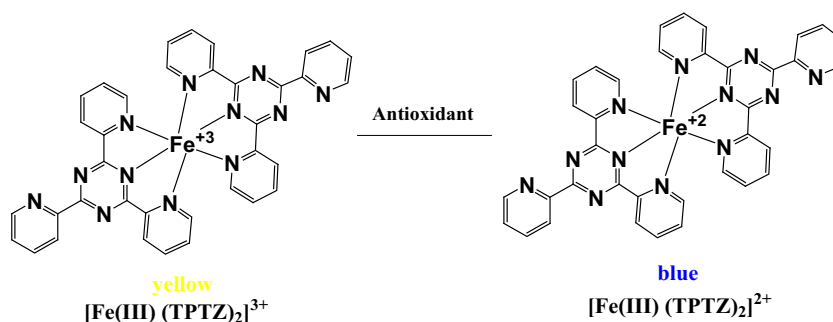
Scheme 2 Redox reaction for ferric complex in the FRAP assay.

Table 3 Reducing power values of the studied compounds.

Compound	equiv. Trolox /10 µM sample (± SD)
1a	130.2 ± 19.7
Caffeic acid 1b	272.7 ± 32.1
Gallic acid 1c	476.8 ± 21.5
Protocatchuic acid 1d	86.8 ± 9.3
3a	205.2 ± 18.6
3b	318.2 ± 68.1
3c	262.4 ± 33.5

All experiments were performed in triplicate. The data are expressed as the mean ± SD of equivalent Trolox/10 µM sample.
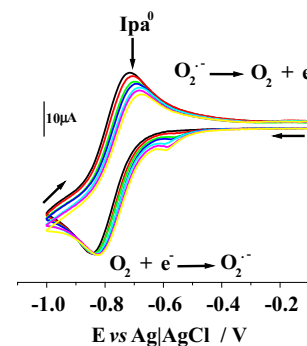

Figure 7a CV for $O_2^{\cdot-}$ redox couple after successively increasing the concentration of compound **1a**. DMF + tetrabuthyl ammonium hexaphluorophosphate (Bu_4NPF_6), 0.2 M; 0.1 V/s.

Figure 7b Dimensionless parameter $(Ip_a^0-Ip_a^S/Ip_a^0)$ *vs* substrate concentration for compound **1a**. (AI_{50} is highlighted in green).

describes the contributions of cyclic voltammetry, differential pulse voltammetry, square wave voltammetry, potentiometry and amperometry in this field (Pisoschi et al., 2015). Several reports show interesting studies in different matrices (Sochor et al., 2013), e.g., beverages (Piljac-Žegarac et al., 2010), vegetables (Zielinska et al., 2008), and *in situ* human skin experiments (Ruffien-Ciszak et al., 2006).

In the scavenging capacity towards superoxide anion, a decrease in oxidation current (Ip_a) was observed after adding a substrate into the working solution (Fig. 7a). The dimensionless parameter ($Ip_a^0-Ip_a^S/Ip_a^0$) was determined, which was plotted against the substrate concentration. For all compounds, a linear correlation with *r*-values of 0.99777–0.97267 was found (Fig. 7b).

From this plot, the antioxidant index 50 (AI_{50}) was obtained, which is the required concentration to reduce the anodic current peak by 50%. In this assay, a lower AI_{50} value corresponds to a larger antioxidant capacity of the substrate against superoxide anion (O_2^-).

As we observed in Table 4, compound **1a** shows higher AI_{50} (0.187 mM) than **3a**, **3b** and **3c**. Thus, we can say that the addition of phenolic substituents into the coumarin scaffold contributes to its antioxidant capacity.

Gallic acid derivative **3b** shows the lowest AI_{50} value; therefore, it is a better quencher to superoxide that forms on the electrode surface, because a low concentration (0.064 mM) was require to decrease Ip_a by 50%. Moreover, this compound presents a potentiation effect against O_2^- with a lower concentration required for radical scavenging than its precursors (**1a** and gallic acid). The second was compound **3c** with an AI_{50} value of 0.137 mM. Finally, derivative **3a** has an AI_{50} value of 0.141 mM. The relative reactivity in this assay was
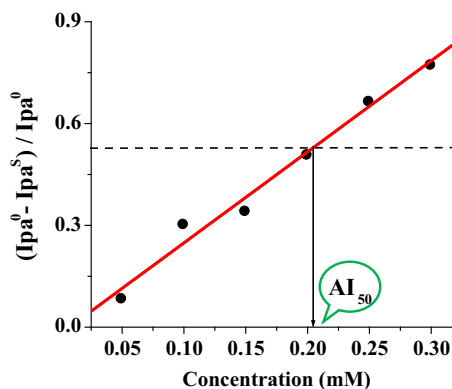
3b > **gallic acid** > **protocatechuic acid** > **caffeic acid** > **3c** > **3a** > **1a**. All compounds had better reactivity than the Trolox standard.

Considering the structures of the compounds, their ability to diffuse from the bulk to the electroactive surface varies. We can compare those with similar structures and molecular weights. In the first group, gallic acid derivative **3b** shows the best AI_{50} value; the compound has more hydroxyl groups in its structure, which increases the polarity in the molecule; the assayed media is aprotic and polar, which enables its best diffusion. The highest value among the derivatives was 0.141 mM

Table 4 AI_{50} values for the superoxide scavenging of all compounds in DMF.

Compound	AI_{50} (mM[b]) (± SD)
1a	0.183 ± 0.007
Caffeic acid 1b	0.125 ± 0.006
Gallic acid 1c	0.104 ± 0.004
Protocatchuic acid 1d	0.115 ± 0.005
3a	0.141 ± 0.011
3b	0.064 ± 0.004
3c	0.137 ± 0.002
Trolox[a]	1.97

[a] Trolox value collected from reference Shirode et al., 2015.
[b] All experiments were performed in triplicate. The data are expressed as the mean ± SD.

Table 5 Cellular antioxidant activity assay of coumarin derivatives at 1 μM and 10 μM.

Compound	% CAA 1 μM	% CAA 10 μM
1a	69.6 ± 5.0	72.7 ± 1.3
Caffeic acid 1b	73.0 ± 2.6	73.9 ± 0.7
Gallic acid 1c	66.2 ± 1.9	70.1 ± 0.1
Protocatechuic acid 1d	47.7 ± 2.5	66.5 ± 2.6
3a	38.1 ± 5.5	49.9 ± 6.6
3b	17.8 ± 4.5	39.5 ± 12.8
3c	34.5 ± 3.1	23.4 ± 10.8

All experiments were performed in triplicate. The data are expressed as the mean ± SD.

Table 6 Retention time values to new derivatives and coumarin precursor.

Compound	Retention time (min)
1a	5.138
3a	5.760
3b	4.031
3c	4.695

Chromatographic conditions: C_{18} ODS Hypersil; the mobile phase was 0.2% orthophosphoric acid solution-acetonitrile (35:65, v/v); isocratic conditions.

for **3a**, which has a double bond, which increases its relative lipophilicity in this medium. The same analysis for the precursor shows that coumarin **1a** has the highest AI_{50} value because the chlorine substituent in the moiety increases its lipophilicity. Gallic acid has the smallest value of 0.104 mM.

This assay provides interesting information about the compound behaviours in non-aqueous media. This environment is a closely similar model to lipid bilayer membranes to investigate oxidative reactions, where dioxygenated reactive species play an important role in the cell redox status (Sawyer et al., 1985; Maricle and Hodgson, 1965).

3.2.5. Evaluation of the antioxidant capacity in EA. Hy 926 (ATCC CRL-2922) cells

To evaluate the antioxidant capacity of coumarin derivatives in a biological model, the probe 2′,7′-dichlorodihydrofluorescein diacetate (DCFH-DA), which diffuses through a cell membrane, was used. In contact with an oxidant (such as an endogenous or exogenous ROS), the dye changes its structure to 2,7-dichlorofluorescein (DCF), which is a fluorescent compound. As described in the literature, this method measures the ability of compounds to avoid DCF formation by AAPH (the peroxyl radical source that we used). The experimental results are shown in Table 5. The results indicate that at both assayed concentrations, derivatives **3a-c** show a poor cellular antioxidant activity (CAA) compared to the precursor scaffold **1a** and hydroxylated acids.

It is worth mentioning that the cell strain for this assay is human (endothelial cells). Unlike murine macrophage cell line models (RAW), this assay provides information regarding the bioavailability of these compounds in an unconventional model (Matos et al., 2015; Mura et al., 2014).

The obtained results in non-biological assays draw attention because the derivatives had better antioxidant capacity than their coumarin precursor. However, in our biological model, we obtained deficient results. Considering that the retention time increases because the compound has higher affinity for the organic stationary phase than the aqueous phase, we determined the relative lipophilicity to compounds **1** and **3a-c** through the retention time by high performance liquid chromatography (HPLC) in a C_{18} column to model the partitioning environment in a reverse phase (Kerns and Di, 2008, Table 6). Additionally, we calculated a correlation between the experimental CAA (10 μM) and the theoretical logD (Fig. 8). This computational tool provides a reliable

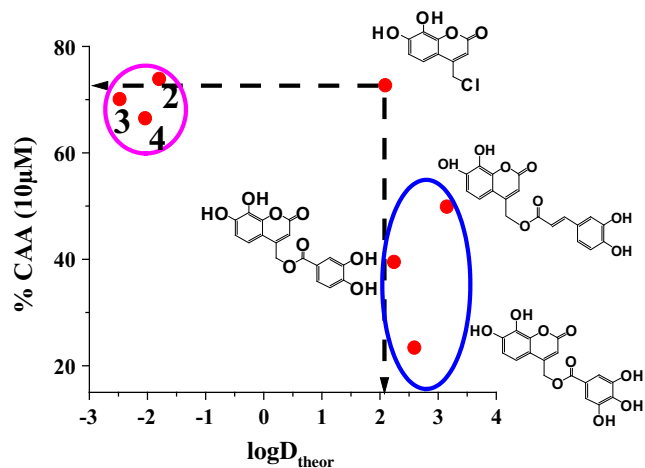**Figure 8** Theoretical correlation of logD vs CAA. logD was calculated using the Marvin Sketch tool from the ChemAxon version 6.3.1 free software[69].

approach about the compound behaviour in lipophilic media (Marvin, ChemAxon).

Fig. 8 shows the correlation of CAA vs logD. First, precursor **1a** had a CAA above 70%, and it was the second one in the relative hydrophobic series with a similar Rt value to the derivative **3a**, which had a lower CAA than 50%. CAA vs logD shows a similar trend, where **1a** has a similar lipophilicity value to the new derivatives but better bioavailability with approximately equal CAA values to those of benzoic acids.

Carboxylesterases are members of the hydrolase family of enzymes. They can hydrolyse functional groups such as amide, ester, and carbamates to their respective acid and alcohol pre-

cursors. This structures are present in different human organs: liver carboxylesterase (hCE1 and hCE2), brain carboxylesterase (hBr2), intestinal carboxylesterase (hiCE, CES2), etc. (Yang et al., 2011; Chen et al., 2013). Wierdl et al., 2008, reported the action of these compounds in the enzyme/prodrug therapy with CTP-11 (7-ethyl-10-[4-(1-piperidino)-1-piperidino]carbonyloxycamptothecin. This compound is a potent antitumor agent activated in cells through the ester cleavage by carboxylesterases. Because the new derivatives are esters, their behaviour in the simple assayed biological model (human intestinal epithelial cells) can be explained by enzymatic degradative phenomena into cells, where carboxylesterases are present in the gastrointestinal tract as a natural barrier to drug absorption (Kerns and Di, 2008).

Benzoic acids and natural polyphenols have high polarity, which limits their bioavailability in non-aqueous media: biomembranes, micelles, emulsions, etc. Ester derivative formation is a common strategy to increase their lipophilicity and obtain "lipophilic antioxidants" with improved characteristics. Tai et al. reported vanillic acid ester derivatives with good ORAC values. Using the OxHLIA assay, they found that their derivatives had a protective effect against free radical-induced erythrocyte membrane damage (Tai et al., 2012).

Another method to increase the polyphenol bioavailability is the encapsulation technology. This strategy enables compound isolation, control of drug delivery, and solving some undesirable characteristics, e.g., their poor water solubility, light or heat sensitivity and low stability (Munin and Edwards-Lévy, 2011).

Micro- or nano-encapsulation methodologies are described in several studies (Pereira et al., 2015; Shirode et al., 2015). A review by Mignet et al. (2013) presents polyphenol liposomal formulations that are proposed to improve the drug delivery for catechin, curcumin, resveratrol, and quercetin. Other studies suggest that the nano-encapsulation of curcumin and gallic acid derivatives is a useful tool to improve their bioavailability and performance in the human body with a focus in colonrectal cancer chemoprevention (Santos et al., 2013).
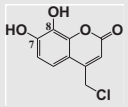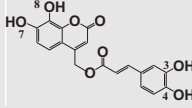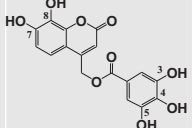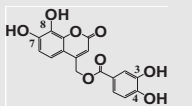
3.2.6. Theoretical studies: Fukui index calculation

To rationalize our experimental results, the Fukui index for oxygen atoms in each synthesized derivative was calculated (Table 7). The values of f^0 (in those atoms in the antioxidant capacity) show that radical attack occurs in different regions of the molecule depending on the derivative. In compound **3a**, the highest Fukui value is at positions 3 and 4 ($f^0 = 0.0389$ and $f^0 = 0.0489$, respectively), which indicates that this site in the molecule has better antioxidant activity than that in coumarin catechol (with Fukui index values of 0.0078 and 0.0021 for O_7 and O_8, respectively). Its behaviour is because the caffeic moiety has a double bond in its structure, which increases the stability of the cation radical phenoxyl (ArO• +) formed as a reaction intermediate.

For compounds **3b** and **3c**, we found that the coumarin moiety was the most reactive region for both molecules. We observe that position 7 was the most reactive position, and position 8 was the second most reactive position in the molecules. Then, catechol from the acid moiety reacts against the radical attack.

These results show that with the Fukui index calculation, we can rationalize the obtained experimental results for the

Table 7 Fukui index and BDE values for the coumarin derivatives.

Compound	Fukui Index f^0	BDE (kcal mol^{-1})
	O_7 **0.0771** O_8 **0.0391**	92.451 96.552
	O_7 0.0078 O_8 0.0021 O_3 **0.0389** O_4 **0.0489**	96.605 95.857 91.908 87.029
	O_7 **0.0719** O_8 **0.0365** O_3 0.0025 O_4 0.0025 O_5 0.0002	89.637 91.162 92.116 96.058 96.973
	O_7 **0.0739** O_8 **0.0378** O_3 0.0004 O_4 0.0003	91.939 89.309 96.562 95.962

Bold values indicate greater reactivity.

synthesized hybrids, which enables us to distinguishing the most reactive region for free radical attacks in molecules with more than one active site (Aliaga and Lissi, 2004).

The antioxidant molecules can act against reactive species by the transfer of hydrogen atoms (HAT) and this capacity can be estimated by the union of values of enthalpy of dissociation (BDE, Pérez-Cruz et al., 2013; Zhu et al., 2010).

The lower of BDE values indicate greater lability of the hydrogen atoms in the hydroxyl groups (Table 7). This is related to a greater antioxidant capacity of the new polyphenolic hybrid-coumarins in relation to the coumarin base. As can be observed, the theoretical results obtained are correlated with the experimental results, such as the ORAC-FL index.

In our study, we found that BDE calculations correlated with Fukui index results. Our calculated bond dissociation energies for O—H group shown that for the compound **3a** the catecol in the caffeic acid moiety has the lowest values in the molecule (91.908 kcal mol^{-1} and 87.029 kcal mol^{-1} for O7 and O8, respectively), thus this is the most reactive site. For compounds **3b** and **3c**, the calculated energies indicate that hydrogen donating ability is in the coumarin catechol. This residue possesses the most available protons, which give the antioxidant capacity to the molecule.

4. Conclusions

In non-biological assays, the inclusion of polyphenolic structures into coumarin improves the antioxidant capacity compared to the **1a** scaffold. A synergy phenomenon was observed in compound **3c** for FRAP and ORAC assays and compound **3b** in the assay of superoxide anion scavenging. In the ESR experiments, we found that all compounds could compete with spin trap to scavenge OH•, which implies that the compounds are potential candidates to reduce the hydroxylradical-induced oxidative damage. The superoxide scavenging results show that compound **3b** is the best molecule of the entire series with an AI$_{50}$ of 0.064 mM. As expected, there is no correlation among the obtained values using different methodologies because of different

oxygen reactive specie (with different reactivity) in each antioxidant assay and medium. In this study, we obtained compounds with better antioxidant capacity than the starter coumarin. Every proposed substitution has better antioxidant activity than the coumarin precursor **1a**. Considering the results in simple biological experiments, new derivatives can exert their antioxidant capacity at the biological level (lipophilic media). Nevertheless, the correlation of logD vs CAA shows that the lipophilicity is not the only factor in the compound behaviour. For our compounds, an encapsulation method can be interesting to attempt. From the theoretical calculations (Fukui index and BDE), we can discriminate different reactive sites in the new molecules where the oxidative process occurs. We found a correlation between both methods: in compound **3a**, the most reactive region in the molecule was the caffeic acid moiety, whereas in compounds **3b** and **3c**, the coumarin scaffold was the active site.

Acknowledgements

References

Abernethy, J.L., 1969. J. Chem. Ed. 46, 561.

Aguirre, P., García-Beltrán, O., Tapia, V., Muñoz, Y., Cassels, B., Nunez, M., 2016. ACS Chem. Neurosci. http://dx.doi.org/10.1021/acschemneuro.6b00309.

Aliaga, C., Lissi, E., 2004. Can. J. Chem. 82, 1668.

Allen, T., Giridhar, M., Razavi, G.J., 2015. J. Cancer Sci. Res. 1, 1.

Asif, M., 2014. Am. J. Curr. Organ. Chem. 1, 1.

Baerends, E., Ellis, D., Ros, P., 1973. Chem. Phys. 2, 41.

Baerends, E., Ros, P., 1978. Int. J. Quantum Chem. 14, 169.

Bauschlicher, C.W., Langhoff, S.R., 1999. Mol. Phys. 96, 471.

Belluti, F., Fontana, G., Dal Bo, L., Carenini, N., Giommarelli, Ch., Zunino, F., 2010. Bioorg. Med. Chem. 18, 3543.

Benzie, I.F., Strain, J., 1996. J. Anal. Biochem. 239, 70.

Biskup, I., Golonka, I., Gamian, A., Sroka, Z., 2013. Postepy Hig. Med. Dosw. 67, 958.

Boerrigter, P., Te Velde, G., Baerends, E., 1988. Int. J. Quantum Chem. 33, 87.

Bolanos de la Torre, A., Henderson, T., Nigam, P., Owusu-Apenten, R., 2015. Food Chem. 174, 119.

Campos-Toimil, M.O., Santana, L., Uriarte, E., 2002. Bioorg. Med. Chem. Lett. 12, 783.

Cao, G., Alessio, H., Cutler, R., 1993. Free Radical Biol. Med. 14, 303.

Carvalho, P., Almeida, L., Araújo, J., Medina, A., Menezes, A., Sousa, J., Oliveira, S., Camargo, A., Napolitano, H., 2016. PLoS ONE 11, 1.

Chamorro, E., Pérez, P., 2005. J. Chem. Phys. 23, 114107.

Chauhan Sh. S., Sharma, M., Prem. Chauhan, M.S., 2010. Drug News & Perspective. 23, 632.

Chen, S., Yueh, M., Bigo, C., Barbier, O., Wang, K., Karin, M., Nguyen, N., 2013. Tukey R H. PNAS 110, 19143.

Cimino, S., Sortino, G., Favilla, V., Castelli, T., Madonia, M., Sansalone, S., Russo, G., Morgia, G., 2012. Oxidative Medicine and Cellular Longevity., ID 632959, http://dx.doi.org/10.1155/2012/632959.

Demircioğlu, Z., Albayrak, Ç., Büyükgüngör, O., 2015. Spectrochim. Acta Part A Mol. Biomol. Spectrosc. 139, 539.

Dua, A., Garg, G., Mahajan, R., 2013. Eur. J. Exp. Biol. 3, 203.

Figueroa, R., Matos, M.J., Vázquez-Rodríguez, S., Santana, L., Uriarte, E., Olea-Azar, C., Maya, J.D., 2013. Future Med. Chem. 5, 1911.

Francl, M., Pietro, W., Hehre, W., Binkley, J., Gordon, M., De Frees, D., Pople, J., 1982. J. Chem. Phys. 77, 3654.

Frisch, M.J., Trucks, G.W., Schlegel, H.B., Scuseria, G.E., Robb, M. A., Cheeseman, J.R., Scalmani, G., Barone, V., Mennucci, B., Petersson, G.A., Nakatsuji, H., Caricato, M., Li, X., Hratchian, H. P., Izmaylov, A.F., Bloino, J., Zheng, G., Sonnenberg, J.L., Hada, M., Ehara, M., Toyota, K., Fukuda, R., Hasegawa, J., Ishida, M., Nakajima, T., Honda, Y., Kitao, O., Nakai, H., Vreven, T., Montgomery, J.A., Peralta, J.E., Ogliaro, F., Bearpark, M., Heyd, J.J., Brothers, E., Kudin, K.N., Staroverov, V.N., Kobayashi, R., Normand, J., Raghavachari, K., Rendell, A., Burant, J.C., Iyengar, S.S., Tomasi, J., Cossi, M., Rega, N., Millam, J.M., Klene, M., Knox, J.E., Cross, J.B., Bakken, V., Adamo, C., Jaramillo, J., Gomperts, R., Stratmann, R.E., Yazyev, O., Austin, A.J., Cammi, R., Pomelli, C., Ochterski, J.W., Martin, R.L., Morokuma, K., Zakrzewski, V.G., Voth, G.A., Salvador, P., Dannenberg, J.J., Dapprich, S., Daniels, A.D., Farkas, Foresman, J.B., Ortiz, J.V., Cioslowski, J., Fox, D.J., Gaussian 09, Revision C.01, in Wallingford CT, 2009.

Furniss, B., Hannaford, A., Smith, O., Tatchell, A., 1948. Vogel's Textbook of Practical Organic Chemistry. John Wiley & Sons, New York, p. 1248.

Gazit, A., Yaish, P., Gilon, Ch., Levitzki, A., 1989. J. Med. Chem. 32, 2344.

Gohari, A.R., Hajimehdipoor, H., Saeidnia, S., Ajani, Y., Hadjiakhoondi, A., 2011. J. Med. Plants 10, 54.

Gülçin, İ., 2006. Toxicology 217, 213.

Gümüş, A., Karadeniz, Ş., Uğraş, H., Bulut, M., Čakir, Ü., Gören, A., 2010. J. Heterocyclic Chem. 47, 1127.

Jayashree, B.S., Nigam, S., Pai, A., Chowdary, P.V.R., 2014. Arab. J. Chem. 7, 885.

Jeong, Ch.-H., Jeong, H.R., Choi, G.N., Kim, D.-O., Lee, U., Heo, H., 2011. J. Chinese Med. 6, 1.

Kakkar, S., Bais, S., 2014. ISRN Pharmacology. ID 952943.

Kale, M., Patwardhan, K., 2014. J. Curr. Pharm. Res. 4, 1150.

Keerthi, M., Lakshmi Prasanna, J., Santhosh Aruna, M., Rama Rao, N., 2014. World J. Pharmacy Pharm. Sci. 3, 445.

Kerns, E., Di, L., 2008. Drug-like Properties Concepts, Structure Design and Methods: from ADME to Toxicity.

Kim, S., Kang, K., Zhang, R., Piao, M., Ko, D., Wang, Z., Chae, S., Kang, S., Lee, K., Kang, H., Kang, H., Hyun, J., 2008. Acta Pharmacol. Sin. 29, 1319.

Kozlowski, D., Trouillas, P., Calliste, C., Marsal, P., Lazzaroni, R., Duroux, J.L., 2007. J. Phys. Chem. A 111 (6), 1138.

Kostova, I., 2006. Mini-Rev. Med. Chem. 6, 365.

Kouznetsov, V.V., Gómez-Barrio, A., 2009. Eur. J. Med. Chem. 44, 3091.

Lattanzio, V., Kroon, P.A., Quideau, S., Treutter, D., 2009. Recent Adv. Polyphenol. Res., 1 chapter 1.

Lazar, C., Kluczyk, A., Kiyota, T., Konishi, Y., 2004. J. Med. Chem. 47, 6973.

Le Bourvellec, C., Hauchard, D., Darchen, A., Burgot, J., Abasq, M., 2008. Talanta 75, 1098.

LeBlanc, L., Paré, A., Jean-François, J., Hébert, M., Surette, M., Touaibia, M., 2012. Molecules 17, 14637.

Li, X., Wang, X., Chen, D., Chen, Sh., 2011. Funct. Foods Health Disease 7, 232.

Link, K., Angell, H., Walker, J., 1929. J. Biol. Chem. 81, 369.

Lopes, A., Macanita, A., Seixas de Melo, J., Martins, A., Pina, F., Wamhoff, H., Melo, E., 1995. Env. Sci. Technol. 29, 562.

Ma, Q., Xi, H., Ma, H., Meng, X., Wang, Z., Bai, H., Wentao, Li, Wang, Ch., 2015. Chromatographia, 78, 241.

Maricle, D.L., Hodgson, W.G., 1965. Anal. Chem. 37, 15162.

Martínez-Araya, J., Salgado-Morán, G., Glossman-Mitnik, D., 2013. J. Chem. http://dx.doi.org/10.1155/2013/850297 Article ID 850297.

Marvin Sketch, software ChemAxon version 6.3.1. < www. chemaxon.com > .

Materska, M., Perucka, I., 2005. J. Agric. Food Chem. 53, 1750.

Matos, M.J., Mura, F., Vázquez-Rodríguez, S., Borges, F., Santana, L., Uriarte, E., Olea-Azar, C., 2015. Molecules 20, 3290.

Meunier, B., 2008. Acc. Chem. Res. 4, 69.

Mignet, N., Seguin, J., Chabot, G., 2013. Pharmaceutics 5, 457.

Munin, A., Edwards-Lévy, F., 2011. Pharmaceutics 3, 793.

Mura, F., Silva, T., Castro, C., Borges, F., Zuñiga, M.C., Morales, J., Olea-Azar, C., 2014. Free Rad. Res. 48, 1473.

Noguer, M., Cerezo, A.B., Moyá, M.L., Troncoso, A.M., García-Parrilla, M.C., 2014. Adv. Chem. Eng. Sci. 4, 258.

Olea-Azar, C., Rigol, C., Mendizábal, F., Briones, R., 2006. Mini Rev. Med. Chem. 6, 211.

Ono, N., Yamada, T., Saito, T., Tanaka, K., Kaji, A., 1978. Bull. Chem. Soc. Japan 51, 2401.

Ou, B., Hampsch-Woodill, M., Prior, R., 2001. J. Agric. Food Chem. 49, 4619.

Parr, R., Yang, W., 1984. J. Am. Chem. Soc. 106, 4049.

Payá, M., Goodwin, P., De las heras, B., Hoult, J.R.S., 1994. Biochemical Pharmacol. 3, 445.

Payá, M., Halliwell, B., Hoult, J.R.S., 1992. Biochem. Pharmacol. 44, 205.

Payá, M., Hoult, J.R.S., 1996. Gen. Pharm.: the Vascular Syst., 27, 713.

von Pechmann, H., 1884. Ber. Dtsch. Chem. Ges. 17, 929.

Pereira, G., Vianello, F., Corrêa, C., da Silva, R., Galhardo, M., 2014. Food Nutr. Sci. 5, 1065.

Pereira, M., Hill, L., Zambiazi, R., Mertens-Talcott, S., Talcott, S., Gomes, C., 2015. LWT - Food Sci. Technol. 63, 100.

Pérez-Cruz, F., Villamena, F.A., Zapata-Torres, G., Das, A., Headley, C.A., Quezada, E., López-Alarcón, C., Olea-Azar, C., 2013. J. Phys. Org. Chem. 26, 773.

Piljac-Žegarac, J., Valek, L., Stipčević, T., Martinez, S., 2010. Food Chem. 121, 820.

Pisoschi, A., Cimpeanu, C., Predoi, G., 2015. Open Chem. 13, 824.

Polovka, M., 2006. J. Food Nutr. Res. 45, 1.

Prior, R., Wu, X., Schaich, K., 2005. J. Agric. Food Chem. 53, 4290.

Pulido, R., Bravo, L., Saura-Calixto, F., 2000. J. Agric. Food Chem. 48, 3396.

Rice-Evans, C., Miller, N., Paganga, G., 1996. Free Rad. Biol. Med. 20, 933.

Ruffien-Ciszak, A., Gros, P., Comtat, M., Schmitt, A., Questel, E., Casas, Ch., Redoules, D., 2006. J. Pharm. Biomed. Anal. 40, 162.

Salikhov, K., Zavoiskaya, N., 2015. Resonance. 963.

Sandhu, S., Bansal, Y., Silakari, O., Bansal, G., 2014. Bioorg. Med. Chem. 22, 3806.

Santos, I., Ponte, B., Boonme, P., Silva, A., Souto, E., 2013. Biotechnol. Adv. 31, 514.

Sawyer, D., Roberts, J., Calderwood, T., Suimoto, H., McDowell, M., 1985. Phil. Trans. R. Soc. London. B. 311, 483.

Sethna, S., Narsinh, S., 1944. Chem. Rev. 1.

Sharma, D., Kumar, S., Makrandi, J., 2011. Green Chem. Lett. Rev. 4, 127.

Shirode, A., Bharali, D., Nallanthighal, S., Coon, J., Mousa, S., Reliene, R., 2015. Int. J. Nanomed. 10, 475.

Sochor, J., Dobes, J., Krystofova, O., Ruttkay-Nedecky, B., Babula, P., Pohanka, M., Jurikova, T., Zitka, O., Vojtech, A., Klejdus, B., Kizek, R., 2013. Int. J. Electrochem. Sci. 8, 8464.

Spasojević, I., Mojović, M., Ignjatović, A., Bačić, G., 2011. J. Serb. Chem. Soc. 76, 647.

Tai, A., Takeshi, Sawano., Ito, H., 2012. Biosci. Biotechnol. Biochem. 76, 314.

Te Velde, G., Baerends, E., 1992. J. Comput. Phys. 99, 84.

Teiten, M.-H., Dicato, M., Diederich, M., 2014. Molecules 19, 20839.

Touaibia, M., Guay, M., 2011. J. Chem. Ed. 88, 473.

Valko, M., Leibfritz, D., Moncola, J., Croninc, M., Mazura, M., Telser, J., 2007. Int. J. Biochem. Cell Biol. 39, 44.

Vázquez-Rodríguez, S., Figueroa-Guíñez, R., Joao, Matos M., Santana, L., Uriarte, E., Lapier, M., Maya, J.D., Olea-Azar, C., 2013. Med. Chem. Commun. 4, 993.

Wang, Y., Avula, B., Dhammika Nanayakkara, N.P., Zhao, J., Khan, I.A., 2013. J. Agric. Food Chem. 61, 4470.

Wierdl, M., Tsurkan, L., Hyatt, J.L., Edwards, C.C., Hatfield, M.J., Morton, C.L., Houghton, P.J., Danks, M.K., Redinbo, M.R., Potter, P.M., 2008. Cancer Gene Ther. 15, 183.

Wojdyło, A., Oszmiański, J., Czemerys, R., 2007. Food Chem. 105, 940.

Wolfe, K., Liu, R.H., 2007. J. Agric. Food Chem. 55, 8896.

Xia, E.-Q., Deng, G.-F., Guo, Y.-J., Li, H.-B., 2010. Int. J. Mol. Sci. 11, 622.

Xu, Sh., Pei, L., Wang, Ch., Zhang, Y.-K., Li, D., Yao, H., Wu, X., Chen, Z.-Sh., Sun, Y., Jinyi, X., 2014. Med. Chem. Lett. 5, 797.

Yang, W., Parr, R., Pucci, R., 1984. J. Chem. Phys. 81, 2862.

Yang, Y., Aloysius, H., Inoyama, D., Chen, Y., Hu, L., 2011. Acta Pharmaceutica Sinica B 1, 143.

Yoshimura, Y., Inomata, T., Nakazawa, H., Kubo, H., Yamaguchi, F., Ariga, T., 1999. J. Food. Agric. Chem. 47, 4653.

Zhu, X.-Q., Wang, Ch.-H., Liang, H., 2010. J. Org. Chem. 75, 7240.

Zielinska, D., Wiczkowski, W., Piskula, M., 2008. J. Agric. Food Chem. 56, 3524.